Applied Energy 89 (2012) 322–328

Contents lists available at ScienceDirect

Applied Energy

journal homepage: www.elsevier.com/locate/apenergy

Effect of heat exchanger material and fouling on thermoelectric exhaust heat recovery

N.D. Love [a,*], J.P. Szybist [b], C.S. Sluder [b]

[a] Department of Mechanical Engineering, 500 W. University Ave., University of Texas El Paso, El Paso, TX 79968, USA

[b] Fuels, Engines, and Emissions Research Center, National Transportation Research Center, 2360 Cherahala Blvd., Knoxville, TN 37932, USA

ARTICLE INFO

Article history:
Received 20 April 2011
Received in revised form 1 July 2011
Accepted 24 July 2011
Available online 23 August 2011

Keywords:
Thermoelectrics
Heat exchanger
Fouling
Exhaust Gas Recirculation
Exhaust
Heat recovery

ABSTRACT

Thermoelectric devices are being investigated as a means of improving fuel economy for diesel and gasoline vehicles through the conversion of wasted fuel energy, in the form of heat, to useable electricity. By capturing a small portion of the energy that is available with thermoelectric devices can reduce engine loads thus decreasing pollutant emissions, fuel consumption, and CO_2 to further reduce green house gas emissions. This study is conducted in an effort to better understand and improve the performance of thermoelectric heat recovery systems for automotive use. For this purpose an experimental investigation of thermoelectrics in contact with clean and fouled heat exchangers of different materials is performed. The thermoelectric devices are tested on a bench-scale thermoelectric heat recovery apparatus that simulates automotive exhaust. It is observed that for higher exhaust gas flowrates, thermoelectric power output increases from 2 to 3.8 W while overall system efficiency decreases from 0.95% to 0.6%. Degradation of the effectiveness of the EGR-type heat exchangers over a period of driving is also simulated by exposing the heat exchangers to diesel engine exhaust under thermophoretic conditions to form a deposit layer. For the fouled EGR-type heat exchangers, power output and system efficiency is observed to be 5–10% lower for all conditions tested.

1. Introduction

Thermoelectric devices are being investigated as a means of improving fuel economy for diesel and gasoline vehicles through the conversion of wasted fuel energy, in the form of heat, to useable electricity. In modern engines 60–85% of fuel energy is expelled as thermal energy in the engine exhaust or radiator systems, and while much of this energy is not available to do work on a 2nd law basis, capturing a small portion of the energy that is available with thermoelectric devices can reduce engine loads and/or alternator size thus decreasing pollutant emissions and fuel consumption [1]. Thermoelectric devices can also be used in conjunction with traditional CO_2 reduction approaches (reducing friction, decreasing pumping losses, and improving combustion efficiencies) to further reduce green house gas emissions [2]. Previous studies have estimated that if the amount of driving energy required for the production of electrical power, approximately 6%, could be recovered this would result in an overall reduction of fuel consumption by 10% [3]. Although challenges exist, it may be possible to recover significant amounts of exhaust waste heat with thermoelectric devices particularly as research of materials and application of heat transfer technologies continue to improve performance of these elements. Continued research in this area is further encouraged as the current national goals and the US Department of Energy's commitment to reducing America's dependence on foreign oil gathers more attention [4].

Several authors have demonstrated the use of thermoelectric elements for automobile heat recovery, installing the devices in the exhaust of vehicles [5–8]. A summary of the aforementioned studies is presented in Table 1. A close look at Table 1 shows that heat recovery efficiencies are low, both on a system basis (<2.5%) and on a thermoelectric generator basis (<3.5%) despite great progress made over the last decade in the thermoelectric materials figure of merit values ZT [9]. The figure of merit value is a non-dimensional number that provides an overall assessment of the thermoelement's electrical conversion efficiency. Although material selection and ZT values are important to the performance of the thermoelectric, power output also greatly depends on the availability of heat in order to maintain a large temperature difference between the hot and cold side materials of the element [9].

1.1. Exhaust heat recovery from EGR coolers

Availability analyses of exhaust through major engine components have been performed previously by Edwards et al. [10,11]. It was discovered that significant amounts of useful work could be recovered offering the potential of large amounts of energy that

* Corresponding author. Tel.: +1 915 747 8981; fax: +1 915 747 5019.
E-mail address: ndlove@utep.edu (N.D. Love).

0306-2619/$ - see front matter © 2011 Elsevier Ltd. All rights reserved.
doi:10.1016/j.apenergy.2011.07.042

Nomenclature

$P_{Element}$	power output from a single thermoelectric device (W)	T_{in}	bulk temperature of air inlet (K)
P_{Total}	total power output of the thermoelectric devices (W)	ZT	thermoelectric figure of merit value (–)
$Q_{Exhaust}$	exhaust gas heat flux (W)	ε	heat exchanger effectiveness (–)
Q_{HX}	heat transferred through heat exchanger walls (W)	η_{HX}	heat exchanger efficiency (–)
$Q_{TE,in}$	heat input to the thermoelectric devices (W)	η_{sys}	overall system efficiency (–)
T_{COLD}	temperature of the cold surface of the thermoelectric device (K)	$\eta_{TE,i}$	energy conversion efficiency of one thermoelectric device (–)
T_{HOT}	temperature of the hot surface of the thermoelectric device (K)		

Table 1
Summary of thermoelectric power outputs, system and thermoelectric efficiencies for various experimental studies.

Ref.	Year	Experimental setup	Test conditions	Element power output (W)	System efficiency (%)	Element efficiency (%)
Takanose and Takamoshi [5]	1993	Gasoline 2 L engine	Tested from Idling to 60–65 km/h hill climb	193 W	2.3	–
Ikoma et al. [6]	1999	Gasoline 2–3 L engine	60 km/h on 3–5% hill climb	130 W	1.1	2.9
Thacher et al. [7]	2007	1999 GMC Sierra pick-up truck 5.8L V8 gasoline engine	112.6 km/h, horizontal road	177 W	–	1.7
Schlichting et al. [8]	2008	1995 Kawasaki Ninja 250R 2-cyl 248 cc	96.6 km/h freeway drive	0.47 W	–	–

could be utilized. An Exhaust Gas Recirculation (EGR) cooler, common on diesel and advanced combustion engines is a well studied and widely used heat rejection unit which can potentially increase thermoelectric device power output as an effective heat exchanger. This paper presents the results of a heat exchanger similar to an EGR cooler used in conjunction with thermoelectric elements. Results from this study are thought to be applicable for either a heat exchanger system in the engine exhaust solely for exhaust heat recovery or thermoelectric devices or implementation of thermoelectric devices onto existing EGR cooling units.

1.2. EGR coolers and exhaust fouling

The heat exchanger design and sizing are critical for automotive applications because while the exhaust system needs to be sized to accommodate full engine load, where the exhaust flows and temperatures are highest, the heat exchanger system needs to function efficiently at low speeds and loads, where light-duty engines typically operate during normal drive cycles. Thus, the heat exchanger system for a thermoelectric exhaust energy recovery system must be designed to perform well over a wide range of exhaust flowrates and temperatures. Previous studies have noted the importance of heat exchanger design and the impact on exhaust heat recovery [5–7].

Exhaust Gas Recirculation (EGR) systems recycle exhaust gases into the engine intake for the purpose of reducing engine-out NO_x emissions. EGR cooling devices enable higher levels of EGR and are becoming standard equipment on modern diesel engines. EGR coolers, however, experience a degradation of heat transfer performance with exposure to engine exhaust, expressed by the heat exchanger effectiveness. This is due to the fouling by the less thermally conductive unburned hydrocarbons and particulate deposits along the heat exchanger surface. Numerous studies have been performed to better understand the effect of fouling on heat and pollutant emission output for these types of heat exchangers. Previous studies are referenced here that highlight the ongoing efforts [12–21]. The thermoelectric elements in the present study will be tested using a heat exchanger similar to an EGR cooler, it is also necessary to account for the fouling effects on the element's power output. Details on the fouling process of the heat exchanger are discussed in later sections. Hence this paper also presents the performance of thermoelectric devices when used with heat exchangers fouled with diesel engine exhaust.

2. Experimental setup and procedure

2.1. Understanding the system

A schematic of the heat flows in a thermoelectric heat recovery system are shown in Fig. 1. A portion of the energy in the engine exhaust is transferred from the gas stream, through the wall of a heat exchanger, through the thermoelectric device, and into the cold-side heat exchanger. A portion of the heat flux through the thermoelectric device is converted to usable electricity. As seen in Fig. 1 a portion of the overall exhaust ($Q_{Exhaust}$) is transferred to the heat exchanger wall (Q_{HX}) while the remaining heat energy (Q) is transferred to other locations along the wall. A portion of Q_{HX} is lost in the wall with some heat reaching the thermoelectric element defined as $Q_{TE,in}$. The thermoelectric device is capable of converting a portion of $Q_{TE,in}$ into usable electricity. The element power output ($P_{Element}$) is proportional to the element efficiency ($\eta_{TE,i}$), surface temperature difference between T_{HOT} and T_{COLD} of the thermoelectric unit, and the figure of merit value (ZT). For this study the ZT value for the elements was 0.73, provided by the manufacturer Marlow Industries Inc. The relationship that describes the thermoelement efficiency, or ability to convert heat to useable electricity, is expressed in the following equation [19]:

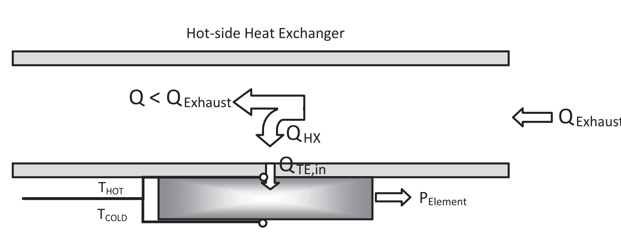

Fig. 1. Heat flow diagram for the hot-side heat exchanger.

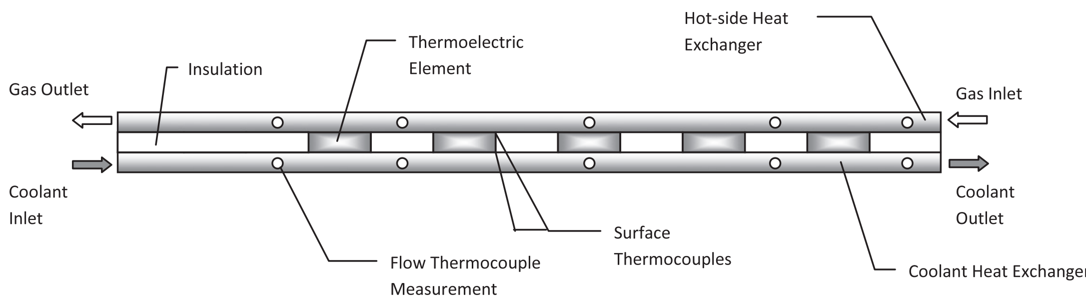

Fig. 2. Schematic diagram of experimental setup.

Table 2
Dimensions of cold and hot-side heat exchangers.

Cold-side heat exchanger	
Length	457 mm
Cross-section	51 mm × 25 mm
Wall thickness	3 mm
Hot-side heat exchanger (stainless steel and aluminum)	
Length	406 mm
Cross-section	51 mm × 25 mm
Wall thickness	3 mm
Circular orifice ports	6.4 mm

$$\eta_{TE,i} = \frac{T_{HOT,i} - T_{COLD,i}}{T_{HOT,i}} * \frac{(1+ZT)^{0.5} - 1}{(1+ZT)^{0.5} + \frac{T_{COLD,i}}{T_{HOT,i}}} \tag{1}$$

Thus by measuring the hot and cold surface temperatures and the power output of each thermoelectric element several parameters can be determined such as: the heat exchanger efficiency (η_{HX}) defined as $Q_{TE,in,total}/Q_{Exhaust}$, the amount of heat transferred to the element, and the overall system efficiency (η_{sys}) shown in the following:

$$\eta_{sys} = \eta_{HX}\eta_{TE,all} = \frac{P_{Total}}{Q_{Exhaust}} \tag{2}$$

where P_{Total} is the total power output of all the thermoelectric elements and $\eta_{TE,all}$ represents the thermoelectric efficiency of all the thermoelectric elements. The heat transfer and efficiency values presented here are used to characterize the system performance and for comparison to previous studies listed in Table 1. A description of the experimental setup and methodologies used to measure the surface temperatures and power output of the thermoelectric devices is given in the following section.

2.2. Thermoelectric experimental setup

The experimental system used in this study is shown schematically in Fig. 2 to detail the position of the hot and cold side heat exchangers, thermocouple positions, and flow directions of the exhaust gas and liquid coolant. The experimental apparatus is composed of three primary sections: (i) cold-side heat exchanger, (ii) hot-side heat exchanger, and (iii) thermoelectric elements.

The cold-side heat exchanger is an aluminum duct with dimensions listed in Table 2. For the cold-side coolant a splash blend of

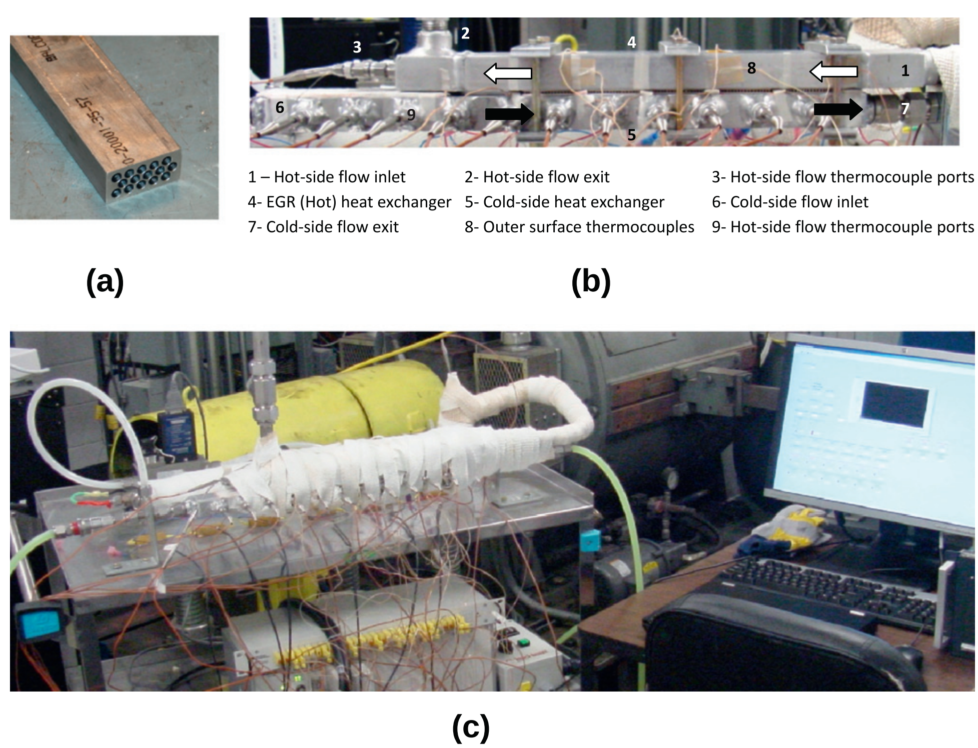

Fig. 3. Digital images showing (a) hot-side heat exchanger cross section, (b) assembled uninsulated experimental setup showing various components, and (c) image of wrapped insulated experimental setup.

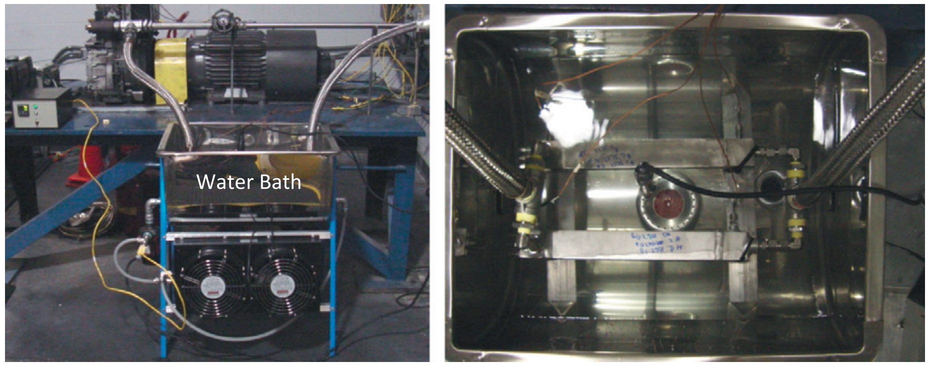

Fig. 4. Heat exchanger fouling setup showing (left) engine, connections, and cooling setup and (right) water submerged EGR cooler heat exchangers.

water and ethylene glycol mixture (50–50 by vol.) is used to simulate vehicle engine coolant. The mixture is delivered from a tank using a 49.7 W pump through Teflon tubing. Temperatures of the coolant mixture are elevated in order to simulate the higher temperatures typically encountered in an automobile radiator with a 1 kW immersion heater used in conjunction with a standard temperature controller. For the hot-side heat exchangers, an EGR-style design is used and the heat exchangers are made from aluminum and stainless steel. Three rows of five columns circular orifice ports arranged in a staggered configuration extended from 50.8 mm to 355.6 mm downstream of the duct inlet, a port arrangement similar to some other previously tested EGR coolers [20]. Temperatures inside of the heat exchanger are monitored with five-insertion style K-type thermocouples inserted through ports located both along the side and near the exit port of the duct. Heated air is delivered to the setup through a 1 kW cartridge connected to a laboratory temperature controller located approximately 550 mm from the first flow thermocouple. A constant hot air flow is maintained with the use of a mass flow controller located approximately 75 mm upstream of the experimental setup. After passing through the apparatus the heated air is discharged to the atmosphere. The hot-side heat exchanger is placed along the top of the cold-side duct with the longer cross section horizontal; dimensions are presented in Table 2. The lower duct is mounted on brackets attached to the inlet and outlet fittings thus eliminating the need for the hot-side to be in contact with an external surface, reducing heat transfer to the surroundings. A counter-flow heat exchanger arrangement is implemented, with the heated air flowing the opposite direction of the liquid coolant as shown in Fig. 3.

Inner surface temperatures of the thermoelectric elements are measured with the use of 12 self adhesive K-type thermocouples placed on the inner portions of both the hot and cold-side heat exchangers (six on both the hot and cold-side). Since placing the thermocouples on the surface of the thermoelectric device can decrease contact area and reduce heat transfer from the hot and cold-side, each is thermocouple is placed directly on either side of each element and the average of the two temperatures for each side taken as T_{HOT} and T_{COLD} in Eq. (1). Unused surface areas and gaps on the heat exchangers are fitted with insulation and the entire apparatus wrapped in laboratory refractory insulation. A photograph of the insulation wrapped experimental setup can be seen in Fig. 3. Five Bi_2Te_3 thermoelectric devices are placed in between the two heat exchangers. To reduce contact thermal resistance of the element, the heat exchanger surfaces are machined smooth, cleaned, and a layer of highly conductive thermal grease is applied to the surface of each device. Each thermoelectric is connected to a 5 Ω power resistor and the output power determined. The wrapped experimental setup showing the configuration of the heat exchangers, thermocouples, clamps, and thermoelectric elements can be seen in Fig. 3. A data acquisition system is used to record the temperatures from the thermocouples and voltage from the five thermoelectric devices simultaneously. The system efficiency is closely monitored and used to determine when the system had reached a steady-state value, defined here as a variation of less than 0.02%. Once steady, data are collected at a sample rate of 1 Hz for 300 s and averaged over this time period.

2.3. Heat exchanger fouling rig

Fouling of the heat exchangers is accomplished by exposing them to diesel engine exhaust under thermophoretic conditions. A bench-mounted naturally aspirated direct-injection single-cylinder diesel engine is used for this study. It has a displacement of 517 cc and a mechanical pump-line-nozzle fuel injection system. The engine is coupled to an electric dynamometer for speed control and to apply load to the engine. This engine platform has been used for numerous previous experimental studies at ORNL, see Ref. [21] for more details.

For this study, the engine is operated at a speed of 1500 rpm and 70% load. The engine exhaust is routed to a pipe tee leading to the aluminum and stainless steel heat exchangers. A pressure of 1.5 psi is maintained in the engine exhaust manifold by manually adjusting a high-temperature gate valve on the engine exhaust bypass. During exposure to engine exhaust, the heat exchangers are submerged in a water bath with a temperature that varied between 50 and 70 °C, conditions that are conducive to thermophoresis. Once steady-state conditions are reached, there is an exhaust temperature reduction in both the aluminum and stainless steel heat exchangers of 130 °C, from 250 °C to 120 °C. The heat exchangers are continuously fouled by the engine exhaust under these conditions for 7 h. The experimental apparatus used to foul the heat exchangers is shown in Fig. 4.

The fouling process accumulated a total soot mass of 1 g in both the aluminum and stainless steel heat exchangers. Assuming that all of the surfaces in the heat exchangers have a uniform soot coating, and the surface area of the heat exchangers inlet and exit portions are accounted for, this amounts to 50–60 mg of soot in each tube of the EGR-style heat exchangers. This is similar soot loading as reported by Sluder et al. [16].

2.4. Experimental test matrix

Table 3 presents the experimental test matrix for the work presented in this paper. Four test conditions are chosen at lower (240 °C) and higher (280 °C) exhaust gas inlet temperatures, selected to be similar to exhaust gas from a diesel engine which ranges from 200 to 700 °C, and lower (40 °C) and higher (80 °C) coolant temperatures. The test matrix is applied to the clean aluminum

Table 3
Experimental test matrix showing the four experimental test conditions repeated for four different heat exchangers.

Condition	Inlet air temperature (°C)	Inlet coolant temperature (°C)
1	240	40
2	280	40
3	240	80
4	280	80

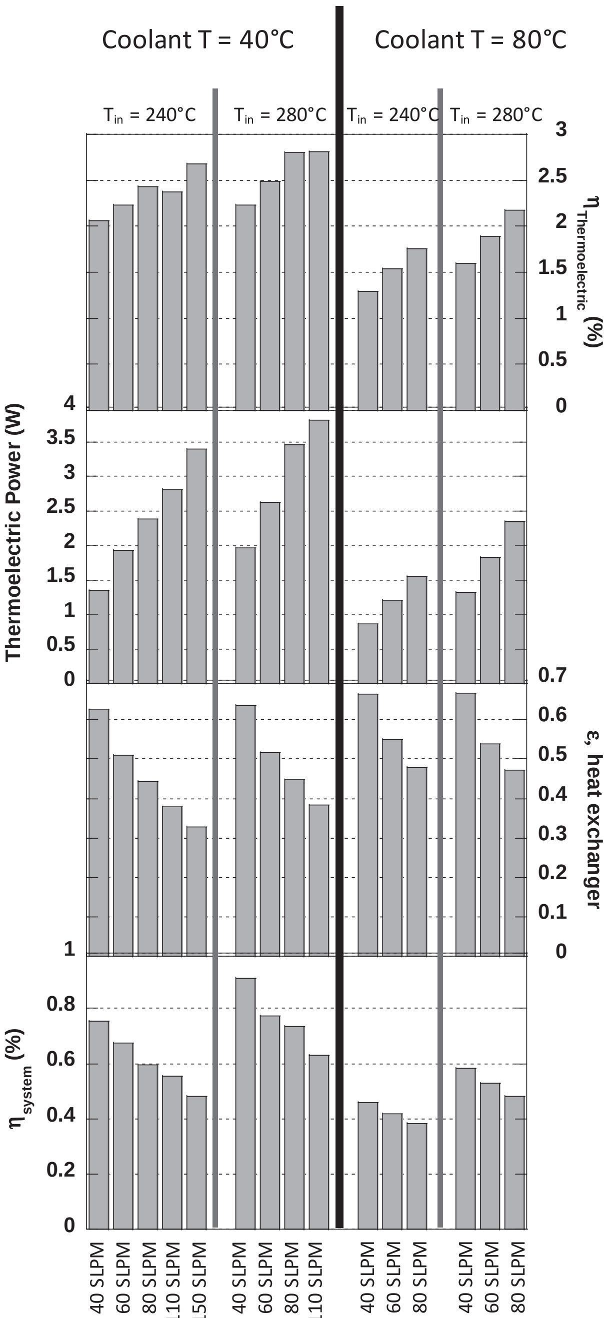

Fig. 5. Response of system efficiency, heat exchanger effectiveness, thermoelectric power, and thermoelectric element efficiency to changing flow and temperature operating conditions the clean aluminum heat exchanger.

and stainless steel heat exchangers, and the fouled aluminum and stainless steel heat exchangers. Each heat exchanger is tested at heat exhaust gas flowrates of 40, 60, and 80 slpm previously verified to produce Reynolds numbers relevant to an automobile engine [19]. Two additional heated exhaust gas flowrates of 110 and 150 slpm are also performed with the clean and fouled aluminum ducts to observe the increase in power of the thermoelectrics at the elevated $Q_{Exhaust}$. The coolant flowrate is kept constant, operating at a full capacity of 126 g/s for all conditions. All measurements are taken at steady state, typically reached after approximately 30 min of either heating or cool-down. Five measurements were taken at each condition and used to estimate the experimental uncertainties which were calculated to be 1.5%, 4.3%, and 4.4% (taken as a percentage of the mean) for η_{sys}, η_{TE}, and P_{Total}, respectively. Experimental uncertainties were calculated using a Student's *t*-test at a 95% confidence level.

3. Results and discussion

Fig. 5 presents the general behavior of the thermoelectric apparatus to changing experimental conditions of η_{TE}, P_{Total}, ε, and η_{sys} for the un-fouled aluminum heat exchanger. The trends observed for this heat exchanger qualitatively represent the trends observed with the stainless steel heat exchanger as well as the fouled heat exchangers. First, it is observed that P_{Total} increases with (1) higher exhaust temperature (280 °C), (2) lower coolant temperature (40 °C), and (3) higher exhaust flow rates. P_{Total} is proportional to the temperature gradient across the thermoelectric devices, and for the first two cases above, the temperature gradient is being directly increased by changing the bulk temperature on either the hot-side or the cold-side of the thermoelectric device. In the third case, a higher flow rate through the heat exchanger increases the amount of available heat. The increased heat transfer at higher flow rates results in increasing thermoelectric efficiency and power output due to higher surface temperatures.

The second observation is that when P_{Total} is increased by using a higher inlet exhaust temperature or a cooler coolant temperature, η_{sys} also increases. However, when P_{Total} is increased by elevating

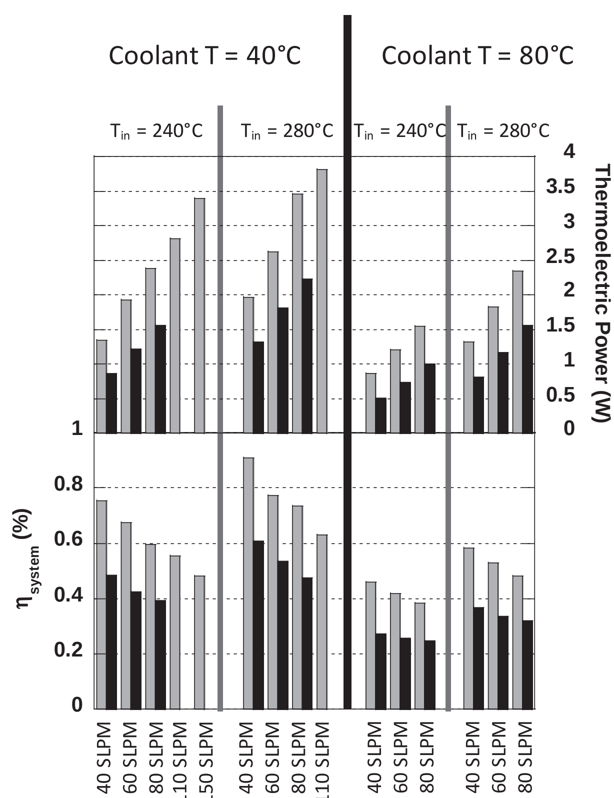

Fig. 6. The effect of heat exchanger material on system efficiency and recovered thermoelectric power for (■) the unfouled aluminum heat exchanger and (■) the unfouled stainless steel heat exchanger.

the exhaust gas flow rate, η_{sys} decreases. The decrease in η_{sys} can be explained by considering the schematic in Fig. 1. By increasing the exhaust flow rate, Q_{HX} is decreased and the heat exiting the EGR-type cooler is higher. The reason for this is that when the gas flow increases for a given set of temperature conditions, heat exchanger effectiveness (ε) decreases substantially, as shown in Fig. 5. Thus when the exhaust flow rate is increased, the temperature gradient across the thermoelectric and P_{Total} both increase, but because ε and subsequently Q_{HX} decreases η_{sys} also decreases.

3.1. Effect of heat exchanger material

Fig. 6 compares η_{sys} and P_{Total} of the unfouled aluminum and stainless steel heat exchangers. At all experimental conditions, P_{Total} was 30–40% lower for the stainless steel heat exchanger compared to the aluminum heat exchanger, with η_{sys} being accordingly higher for the aluminum heat exchanger. The reason for this difference is that the thermal conductivities of stainless steel and aluminum are approximately 15 W/m K and 237 W/m K, respectively [22], thus the thermal resistance is substantially higher in the stainless steel heat exchanger. This also illustrates that the heat exchangers used for this study were non-ideal because of the excessive material thickness in the heat exchanger itself, approximately 4 mm. Ideally, the heat exchanger material would sufficiently thin so that the effect of the material on overall performance is small or negligible. Thus because the stainless steel heat exchanger has a lower thermal conductivity and because of the thickness of the heat exchanger material, the heat flux to the thermoelectric generator is substantially lower for the stainless steel heat exchanger.

3.2. Effect of heat exchanger fouling

The effect of heat exchanger fouling on η_{sys} and P_{Total} is shown in Fig. 7 for the aluminum heat exchanger and in Fig. 8 for stainless steel. Both the aluminum and stainless steel heat exchangers exhibit a similar response, namely that both η_{sys} and P_{Total} decreased for the fouled heat exchangers. The decrease in P_{Total} was generally 5–10% compared to the unfouled heat exchanger for both aluminum and the stainless steel. The overall effect of the heat exchanger material relative to the effect of heat exchanger fouling can be seen for $Q_{TE,in}$ in Fig. 9. Heat exchanger fouling does decrease the heat flux to the thermoelectric devices, but heat exchanger material has a larger impact.

While η_{sys} and P_{Total} are both consistently lower at all experimental conditions for the fouled heat exchangers, the magnitude

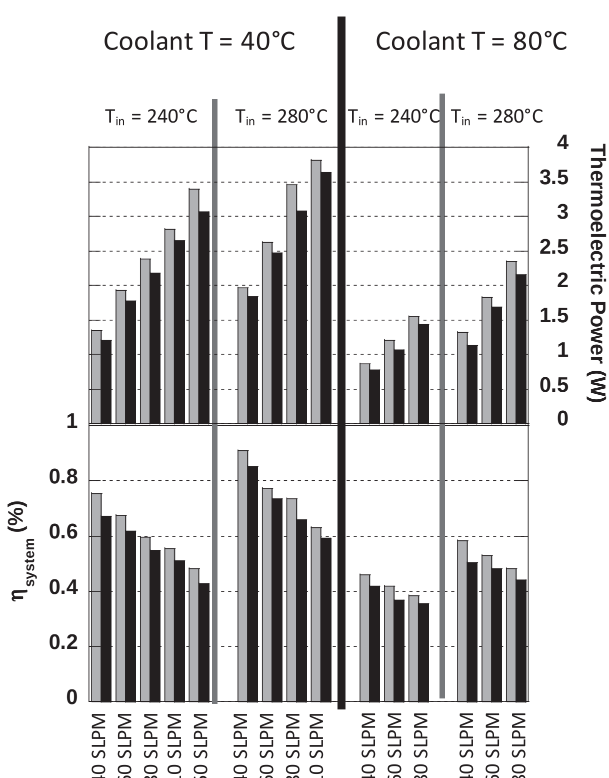

Fig. 7. The effect of heat exchanger fouling on system efficiency and thermoelectric power for (■) the unfouled aluminum heat exchanger and (■) the fouled aluminum heat exchanger.

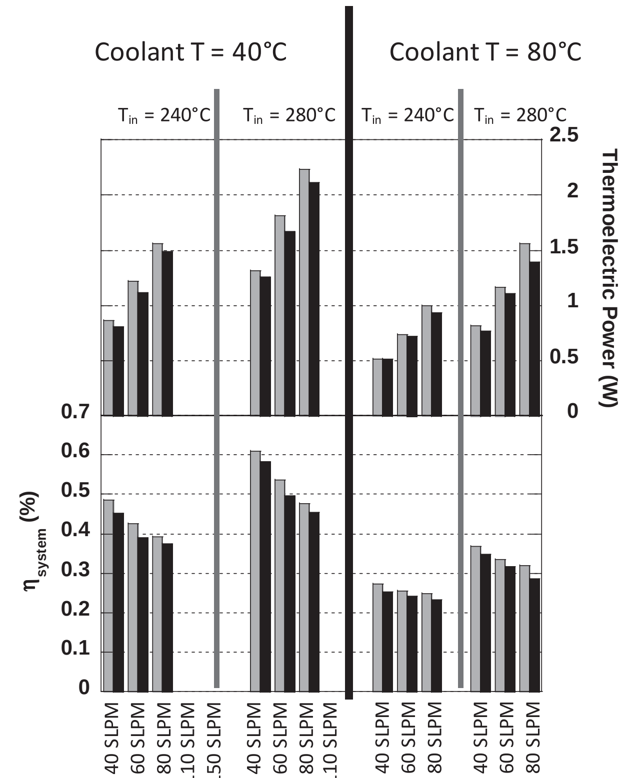

Fig. 8. The effect of heat exchanger fouling on system efficiency and thermoelectric power for (■) the unfouled stainless steel heat exchanger and (■) the fouled stainless steel heat exchanger.

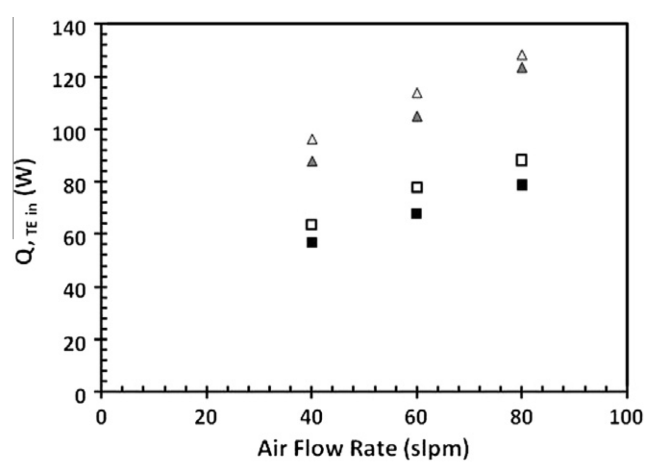

Fig. 9. Heat captured by the thermoelectric where ■ = Fouled stainless steel, □ = Clean stainless steel, ▲ = Fouled aluminum, and △ = Clean aluminum EGR heat exchangers for condition 2 at 40, 60, and 80 slpm.

of the difference is smaller than was initially expected based on previous EGR cooler fouling experiments by Sluder et al. [16]. Considering both the thermal conductivity and the thickness of the deposits a better understanding of the discrepancy can be achieved. Hoard et al. [20] provides a comprehensive literature review of thermal conductivities of deposits on various parts of the engine including intake systems, combustion chambers, and particulate filters. All deposits had very low thermal conductivities, with values ranging from 0.15 to 0.68 W/m K. Sluder et al. [16] found that even a small layer of deposit could substantially reduce the heat exchanger effectiveness when the heat exchanger wall was thin, 0.71 mm. In this study we estimate deposit thickness on the walls of the heat exchangers to be 0.1 mm compared to 4 mm for the heat exchanger wall thickness. The thickness of the deposit layer is calculated based on the tube dimensions, mass of deposited particulate matter, and assumed as having a soot density of 50 kg/m^3, a value taken from Hoard et al. [20]. Thus, even though the deposit layer does affect the heat exchange process, the heat exchanger material thickness dominates the overall heat exchange behavior of this system. The impact of heat exchanger fouling is expected to have a larger impact on η_{sys} and P_{Total} in a heat exchanger system that is more optimally designed with thinner heat exchanger walls.

4. Conclusion

Clean and fouled aluminum and stainless steel EGR-style heat exchangers have been tested on a bench-scale thermoelectric apparatus to simulate automotive exhaust heat recovery. The thermoelectric devices were tested with different hot-side stainless steel and aluminum EGR-type heat exchangers for various heated exhaust gas flowrates ranging from 40 to 150 slpm, exhaust gas temperatures of 240 °C and 280 °C, and coolant side temperatures of 40 °C and 80 °C simulating possible temperature ranges downstream of the engine manifold and engine coolant. From analysis of the results it was observed that the recovered electrical power of the thermoelectric devices can be increased by elevating the temperature of the exhaust gas, decreasing the temperature of the coolant, or by increasing the flow rate of the heated gas. System efficiency increases with an increase in electrical power when the bulk temperature gradient increases. System efficiency decreases with an increase in electrical power when the exhaust gas flow rate is increased. A large effect of heat exchanger material was also documented in this study. This is thought to be a combined effect of the higher thermal conductivity of aluminum compared to stainless steel, and the excessive wall thickness of the heat exchangers used in this study. A more optimally designed heat exchanger would likely be less sensitive to heat exchanger material. Heat exchangers fouled with diesel exhaust experience a degradation in performance of 5–10% compared to an unfouled heat exchanger of the same material.

Acknowledgements

The authors would like to thank the laboratory directed research and development program at Oak Ridge National Laboratory where this work was performed under Project L05394 'Variable valve actuation to enable highly efficient engines'. N. D. Love would like to express appreciation of financial support through an Oak Ridge Associated Universities Historically Black Colleges and Universities and Minority Educational Institutions.

References

[1] Stabler F. Automotive applications for high efficiency thermoelectrics. High Efficiency Thermoelectric Workshop; 2002.
[2] Mori M, Yamagami T, Oda N, Hattori M, Sorazawa M, Haraguchi T. Current possibilities of thermoelectric technology relative to fuel economy. Soc Autom Eng 2009;2009:01–0170.
[3] Vazquez J, Sanz-Bobi M, Palacios R, Arenas A. State of the art of thermoelectric generators based on heat recovered from the exhaust gases of autombiles. In: Proceedings of the seventh European workshop on thermoelectrics; 2002.
[4] Department of Energy. <http://www.energy.gov/energyefficiency/index.htm>, July 2010.
[5] Takanose E, Tamakoshi H. The development of thermoelectric generator for passenger car. In: Proceedings of the 12th IEEE international conference on thermoelectrics; 1993. p. 467–70.
[6] Ikoma K, Munekiyo M, Furuya K, Kobayashi M, Izumi T, Shinnohara K. Thermoelectric generator for gasoline engine vehicles using Bi_2 Te_3 modules. J Japan Inst Metals 1999;63(11):1475–8.
[7] Thacher E, Helenbrook B, Karri M, Richter C. Testing of an automobile exhaust thermoelectric generator in a light truck. Proc Inst Mech Eng D J Auto Eng 2007;221:95–107.
[8] Schlichting A, Anton S, Inman D. Motorcycle waste heat energy harvesting. In: Proceedings of the SPIE industrial and commercial applications of smart structures technologies; 2008. p. 6930.
[9] Fairbanks J. Thermoelectric applications in vehicles status 2008. In: Proceedings of the 6th European conference on thermoelectrics. ICMPE-CRNS; 2008. p. 1–8.
[10] Edwards K, Wagner R, Graves R. Identification of potential efficiency opportunities in internal combustion engines using a detailed thermodynamic analysis of engine simulation results. Soc Automot Eng (SAE), Paper 2008-01-0293.
[11] Edwards K, Wagner R, Briggs T. Investigating potential light-duty efficiency improvements through simulation of turbo-compounding and waste-heat recovery systems. Soc Automat Eng 2010. 01-2209.
[12] Zhang R, Charles F, Ewing D, Chang J, Cotton J. Effect of diesel soot deposition on the performance of exhaust gas recirculation cooling devices. Soc Automot Eng 2004. 01-0122.
[13] Bravo Y, Lazaro J, Garcia-Bernad J. Study of fouling phenomena on EGR coolers due to soot deposits: development of a representative test method. Soc Automot Eng 2005. 01-1143.
[14] Charles F, Ewing D, Becard J, Chang J, Cotton J. Optimization of the exhaust mass flow rate and coolant temperature for exhaust cooling devices used in diesel engines. Soc Automot Eng 2005. 01-0654.
[15] Ismail B, Charles F, Ewing D, Cotton J, Chang J. Mitigation of the diesel soot deposition effect on the exhaust gas recirculation (EGR) cooling devices for diesel engines. Soc Automot Eng 2005. 01-0656.
[16] Sluder C, Storey J, Youngquist A. ULSD and B20 hydrocarbon impacts on EGR cooler performance and degradation. Soc Automot Eng 2009. 01-2802.
[17] Bravo Y, Moreno F, Longo O. Improved characterization of fouling in cooled EGR systems. Soc Automot Eng 2007. 01-1257.
[18] Ishikawa N, Ohkubo Y, Kudou K. Study on the effects of EGR cooler performance on combustion properties of the pre-mixed compression ignition combustion by multi cylinder DI diesel engine. Soc Automot Eng 2007. 01-1881.
[19] Ibrahim E, Szybist J, Parks J. Enhancement of automotive exhaust heat recovery by thermoelectric devices. Proc Inst Mech Eng D J Auto Eng 2010;224:1–15.
[20] Hoard J, Abarham M, Styles D, Giullano J, Sluder C, Storey J. Diesel EGR cooler fouling. Soc Automot Eng 2008. 01-2475.
[21] Youngquist A, Nguyen K, Bunting B, Toops T. Development of an accelerated ash loading protocol for diesel particulate filters. Soc Automot Eng 2008. 01-2496.
[22] Cengel Y. Heat and Mass Transfer a Practical Approach. 3rd ed. New York: McGraw-Hill; 2006.